JCTC Journal of Chemical Theory and Computation

Article

pubs.acs.org/JCTC

Oxidation States from Wave Function Analysis

Eloy Ramos-Cordoba, Verònica Postils, and Pedro Salvador*

Institut de Química Computacional i Catàlisi (IQCC) i Department de Química, Universitat de Girona, 17071 Girona, Spain

Supporting Information

ABSTRACT: We introduce a simple and general scheme to derive from wavefuntion analysis the most appropriate atomic/fragment electron configurations in a molecular system, from which oxidation states can be inferred. The method can be applied for any level of theory for which the first-order density matrix is available, and unlike others, it is not restricted to transition metal complexes. The method relies on the so-called spin-resolved effective atomic orbitals which for the present purpose is extended here to deal with molecular fragments/ligands. We describe in detail the most important points of the new scheme, in particular the hierarchical fragment approach devised for practical applications. A number of transition metal complexes with different formal oxidation states and spin states and a set of organic and inorganic compounds are provided as illustrative examples of the new scheme. Challenging systems such as transition state structures are also tackled on equal footing.

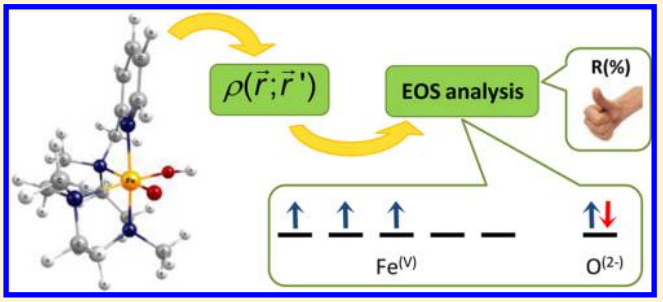

1. INTRODUCTION

The concept of formal oxidation state is widespread in transition metal chemistry and in the study of redox and catalytic reactions. The reactivity, spin state, spectroscopic, and geometrical features of transition metal (TM) complexes are often rationalized on the basis of the oxidation state of the metal center. In coordination chemistry, the so-called oxidation number is defined as *the charge left on the central atom after removing all ligands along with the electron pairs they share with it*. In general, oxidation states (OS) are obtained by assigning an integer number of electrons to the atoms/ligands according to some rules. However, in complicated bonding situations involving noninnocent ligands or in intermediates or transition states of reactions, the formal OS assignments may be rather ambiguous. Doubtless there is need for computational approaches to deal with such difficult cases.

OS are intrinsically related to electronic distribution, but the atomic charge after the formal electron counting is only imaginary. Electronic populations do change with oxidation/reduction of the metal center, but they are only a pointer of the OS.[1,2] Even spin populations need a previous knowledge of the electronic structure (spin state),[3] and are futile for pure singlet states, for which the spin density vanishes.

Empirical methods such as the bond valence sum model[4] can provide estimates of the oxidation states of TM complexes from the molecular geometry. On the other hand, there have been several attempts to derive OS from first principles. Sit et al.[5] used projection techniques to obtain d-orbital populations of the central metal atom in TM complexes. Knizia applied the same approach using a different set of reference d-orbitals.[6] Unfortunately, the method is limited to TM complexes and cannot deal with metal−metal bonds. Thom et al.[3] applied population analysis over localized orbitals to assign individual electrons to atoms according to a threshold. Sit et al.[7] introduced another interesting approach for plane-wave calculations in which the position of the centers of gravity of maximally localized Wannier functions was used to assign the electrons to the closest center.

In this work, we wish to take a somewhat different approach to the problem by focusing on the most appropriate definition of the *effective* electronic configuration of the atoms/fragments within a molecular system. For this purpose, one needs, first of all, to rely on some sort of natural-type atomic orbitals and their occupancies. There are a number of approaches in the literature that provide natural-type atomic orbitals.[6,8−19] For the present purpose, one of the necessary features is that the natural-type atomic orbitals must exhibit (in terms of occupation numbers) a clear-cut separation between the occupied and virtual atomic orbitals. For instance, Cioslowski's atomic orbitals[14] in molecules (AOIM), which exhibit a number of interesting properties, would not be adequate for the present purpose. The method should be applicable on equal footing for any level of theory. Some approaches that focus on the concept of minimal atomic basis[6,16−18] are essentially applicable for mean-field theories. Also, it should not depend upon the nature of the underlying basis set, that is, be applicable when core potentials are used or the molecular orbitals are expanded over plane waves.[20,21] Finally, definitions of functional groups/molecular fragments should be possible within the formalism.

In our opinion, the most appropriate tools for the present purpose are the so-called effective atomic orbitals[8,12,13,15,22] (henceforth eff-AOs). In this approach, the *net* atomic population is expressed in terms of an orthonormal set of

Received: December 3, 2014
Published: February 20, 2015

DOI: 10.1021/ct501088v
J. Chem. Theory Comput. 2015, 11, 1501−1508

hybrids and their occupation numbers. The shape and occupation number of the hybrids faithfully reproduce the core and valence shells of the atoms; those with occupation numbers close to 2 are associated with core orbitals or lone pairs, whereas those with smaller but significant occupation are identified with the atomic orbitals directly involved in the bonds. The remaining eff-AOs are marginally occupied and have no chemical significance. For most atoms, the number of hybrids with significant occupation number always coincide with the classical minimal basis set, except for those that exhibit hypervalent character.[13]

In this work, we will show how formal oxidation states can be easily derived in a general manner from the proper analysis of the occupation numbers of the eff-AOs of individual atoms or molecular fragments. In the next section, we will briefly review the formalism of the eff-AOs. Then, we will describe a hierarchical fragment approach devised for practical applications of the scheme, as well as several illustrating examples.

2. SPIN-RESOLVED EFFECTIVE ATOMIC ORBITALS

Let us consider a spin-unrestricted single-determinant wave function built from n_σ singly occupied molecular orbitals (MOs), $\{\varphi_i^\sigma(\vec{r})\}_{i=1,n_\sigma}$, where $\sigma = \alpha, \beta$. For each atom A of the molecule, one can define the intra-atomic part or every MO as

$$\varphi_i^{A,\sigma}(\vec{r}) \equiv \varphi_i^\sigma(\vec{r}) w_A(\vec{r}) \tag{1}$$

where $w_A(\vec{r})$ is a non-negative weight function satisfying the requirement $\sum_A w_A(\vec{r}) = 1$, which defines the fuzzy domain of atom A in the molecule. For each spin case, one can build a $n_\sigma \times n_\sigma$ overlap matrix of the intra-atomic MOs, $\mathbf{Q}^{A,\sigma}$, with elements

$$Q_{ij}^{A,\sigma} = \int \varphi_i^{A,\sigma *}(\vec{r}) \varphi_j^{A,\sigma}(\vec{r})\, \mathrm{d}\vec{r} \tag{2}$$

The hermitian matrix $\mathbf{Q}^{A,\sigma}$ is diagonalized by the unitary matrix $U^{A,\sigma}$

$$\mathbf{U}^{A,\sigma\dagger}\mathbf{Q}^{A,\sigma}\mathbf{U}^{A,\sigma} = \mathrm{diag}\{\lambda_i^{A,\sigma}\} \tag{3}$$

The normalized spin-resolved eff-AOs for atom A are obtained as a linear combination of the intra-atomic part of the MOs as

$$\chi_i^{A,\sigma}(\vec{r}) = \frac{1}{\sqrt{\lambda_i^{A,\sigma}}} \sum_\mu^{n_\sigma} U_{\mu i}^{A,\sigma} \varphi_\mu^{A,\sigma}(\vec{r}) \qquad i = 1, n_\sigma^A \tag{4}$$

where n_σ^A is the number of nonzero eigenvalues $\lambda_i^{A,\sigma}$. The latter are the corresponding occupation numbers of the spin-resolved eff-AOs,[23] with $0 < \lambda_i^{A,\sigma} \leq 1$.

We have just described how the eff-AOs are obtained in the framework of 3D-space analysis, rendered by the atomic weight functions.[15] A remarkable feature of the eff-AOs is that they can be derived for essentially any atom in molecule definition. Indeed, they were originally derived for Mulliken-type approaches,[12] and later reformulated for the quantum theory of atoms in molecules (QTAIM)[13,22] 3D-space partitioning. The chemical picture emerging from the eff-AOs is virtually independent of the underlying atomic definition used. The shape of the highly occupied hybrids does not change significantly, and only the occupation numbers exhibit some differences. For instance, in Mulliken-type Hilbert-space analysis, the occupation numbers $\lambda_i^{A,\sigma}$ are not strictly restricted to the $0 \leq \lambda_i^{A,\sigma} \leq 1$ range so that 3D-space analysis appears to be more appropriate from a conceptual perspective. For nonoverlapping atomic domains such as in QTAIM, the eff-AOs have special properties; e.g., the eff-AOs on different atoms form a (numerical) atomic basin-centered orthogonal basis set and the occupation numbers do add up to the total number of electrons in the system.[22] These last two properties are also fulfilled by the Löwdin-type Hilbert-space eff-AOs, introduced in this work and described in the Appendix.

Another relevant aspect is that the eff-AOs can be easily obtained for any level of theory, provided a first-order density matrix is available (in the case of the Kohn−Sham DFT, the latter is approximated by the usual HF-like expression).[15] As noted by Mayer,[13] the eff-AOs of a given atom A can also be obtained from the diagonalization of the matrix $\mathbf{PS}^A$, where $\mathbf{P}$ is the LCAO density matrix and $\mathbf{S}^A$ is the intra-atomic overlap matrix in the actual (AO or MO) basis. This permits the straightforward generalization to correlated wave functions, from which the $\mathbf{P}$ matrix is usually available. Moreover, since they can be derived from the intra-atomic part of the density but in the MO basis, they can also be obtained even in the absence of an underlying atom-centered basis set, i.e., for a plane wave calculation.[21]

3. EFFECTIVE OXIDATION STATES ANALYSIS

The fundamental part of the present approach is how to use the information provided by the eff-AOs and their occupation numbers in order to derive the most appropriate electron configuration of the atoms/fragments within the molecule. The easiest avenue would be simply to round up the occupation numbers of the eff-AOs to the nearest integer. Such a naïve approach has several drawbacks that make it inapplicable. First of all, by doing the rounding process for all centers, one may end up with a different number of electrons than were originally in the molecule (typically less because the sum of the net populations is smaller than the number of electrons). Second, the values of the occupation numbers may differ from one atomic definition to another, leading to an undesired strong dependence upon the particular atomic definition used in the eff-AO construction. And last but not least, the effective electron configuration of a given atom within a molecule necessarily affects that of the remaining atoms, as the (integer) electrons need to be redistributed.

Thus, it appears more appropriate to distribute the electrons among the atoms by *comparing* the occupations of the eff-AOs on different atoms, rather than independently rounding them. Moreover, in order to conserve the number of alpha and beta electrons in the process, one should obtain the eff-AOs associated with the alpha and beta intra-atomic density separately. The proposed strategy is (i) to collect the alpha eff-AOs that are significantly populated for *all* centers, (ii) to sort them according to decreasing occupation number, and (iii) to assign integer alpha electrons to the eff-AOs of the centers with higher occupation number, until the number of alpha electrons is reached. Then, proceed analogously for the beta electrons. By this procedure, an effective electronic configuration is obtained for each atom. The effective oxidation state (EOS) of each atom is simply given by the difference between its atomic number and the number of alpha and beta electrons that have been assigned to it. Note that the EOS of a given atom does not only depend upon the population of its eff-AOs but also on that of the remaining atoms, and of course on the total number of alpha and beta electrons of the molecule. This scheme can be applied to basis sets including effective core

DOI: 10.1021/ct501088v
J. Chem. Theory Comput. 2015, 11, 1501−1508

potentials. Simply, the electrons described by the atomic core potential are assigned to the given atom, and then removed from the number of alpha and beta electrons that are distributed in steps i–iii.

In addition, the occupation numbers of the *frontier* eff-AOs, namely, the last occupied, $\lambda^{\sigma}_{\mathrm{LO}}$, and the first unoccupied, $\lambda^{\sigma}_{\mathrm{FU}}$, eff-AOs, can be used to indicate how close the formal picture given by the EOS is to the actual electronic distribution of the system. Ideally, these occupations should be close to 1 and 0, respectively, but such values are only expected for noninteracting atoms. In practice, the atoms share the electrons and this is clearly reflected in the relative occupation numbers of their eff-AOs. Since the EOS are determined by integer electrons, we assume that when $\lambda^{\sigma}_{\mathrm{LO}}$ and $\lambda^{\sigma}_{\mathrm{FU}}$ differ by more than *half* an electron (i.e., a full electron rounding up the difference in occupation number) the assignation of EOS is considered as indisputable. Thus, from the occupation numbers of the *frontier* eff-AOs, one can derive a simple global index to quantify how reliable the formal picture of the oxidation states is. For each spin case, one can compute the following quantity

$$R_{\sigma}\ (\%) = 100 \min(1, \max(0, \lambda^{\sigma}_{\mathrm{LO}} - \lambda^{\sigma}_{\mathrm{FU}} + 1/2)) \qquad (5)$$

and then $R = \min(R_{\alpha}, R_{\beta})$; that is, the overall R index is the minimum value obtained for either the alpha or beta electrons. The larger the R value, the closer the overall assignation of the EOS is to the actual electronic structure of the system. Note that R can take values formally from 0 to 100%, where values below 50% indicate that the assignation of the electrons has not followed an *aufbau* principle according to the occupation numbers of the eff-AOs. The latter can be used to answer the question *how does the system conform with a given set of oxidation states*, rather than *which are the most appropriate formal oxidation states* for the system.

In some occasions, it may occur that the frontier eff-AOs are degenerated due to symmetry, which in principle would yield a R value of 50%, the worst case scenario. In that case, however, one may choose to assign a half-electron to each of the two centers involved, so that both degenerated eff-AOs are considered as occupied. Note that for spin-restricted wave functions this is essentially equivalent to assigning the alpha electron to one center and the beta electron to the other (e.g., for symmetric bis radical ligand metal complexes, see below). For mixed-valence complexes in general, such as in the $[Cu_3S_2]^{2-}$ core,[24] one can either assign noninteger electrons to the center with (near) degenerate eff-AOs or follow steps i–iii, thus selecting one of the possible alternatives with integer oxidation states. The second option is probably more appropriate for electron delocalized systems.[25] Nevertheless, for these particular cases, the designation of EOS is somewhat ambiguous.

4. HIERARCHICAL FRAGMENT/LIGAND APPROACH

Practical applications of the method may involve reaction intermediates or transition state (TS) structures of complexes exhibiting bulky and/or noninnocent ligands. When the number of atoms of the system is large, accidental pseudodegeneracies of the occupation numbers of the eff-AOs are likely to occur, which makes the assignation of EOS difficult. Also, in most cases, one is merely interested in the oxidation state of the TM atoms and the formal charge of the ligands, and not necessarily that of all atoms forming them. In particular, when the latter include hydrocarbyl groups or units exhibiting extremely apolar bonds, the mere concept of formal charges is doubtful (and establishes the limit of applicability of the present approach, as shown in the last section).

A slightly more involved but more efficient strategy is a hierarchical approach, by which molecular fragments are defined *before* the eff-AO analysis in a first iteration. That is, instead of eff-AOs, we obtain effective fragment orbitals by using in eq 1 fragment weight functions of the form

$$w_K(\vec{r}) = \sum_{i \in K} w_i(\vec{r}) \qquad (6)$$

where the sum runs for all atoms of molecular fragment K. In TM complexes, the fragments are typically identified with the metal atom, the ligands, and the molecular species that may be present, such as reactants or explicit solvent molecules, if any. Then, steps i–iii described above lead to the proper distribution of the electrons of the system among the different fragments. In a second iteration, if necessary, the EOS of the individual atoms (or subfragments such as functional groups) forming a fragment can be derived by computing their eff-AOs and by distributing only the alpha and beta electrons that were assigned to the fragment in the first iteration, following again steps i–iii.

One can anticipate that when the identification of the fragments is disputable (e.g., presence of stretched bonds or atomic clusters) different EOS might be obtained for different fragment definitions. In this case, the values of the R index can be very useful to establish the most appropriate chemical picture emerging from the analysis.

5. COMPUTATIONAL DETAILS

The wave function and electron densities of all systems have been computed at the UB3LYP/6-31G* level of theory (unless otherwise stated) using the Gaussian 03 package.[26] The spin-resolved effective atomic orbitals (eff-AOs) and effective oxidation states (EOS) have been obtained with the APOST-3D program,[27] using a 70 × 434 atomic grid for the numerical integration. The topological fuzzy Voronoi cells (TFVC) atomic definition[28] was used throughout with a threshold on the eff-AO occupations of 0.01 (i.e., eff-AOs with occupation numbers below the threshold were ignored), unless otherwise stated.

6. ILLUSTRATIVE EXAMPLES

We have considered a number of examples to show the usefulness of the present approach. First of all, we have carried out a systematic study of a series of octahedral TM complexes with different ligands and a well-established metal oxidation state. The same set was used by Thom et al. for the calibration of their localized orbital bond analysis scheme.[3] The results are gathered in Table 1.

The computed EOS for the central metal atom are in agreement with the chemically expected values in all cases, with high values of the R index. The analysis also yielded EOS of $(H^{(+)})_2O^{(2-)}$, $C^{(2+)}N^{(3-)}$, and $C^{(2+)}O^{(2-)}$ for the H_2O, CN^-, and CO ligands, respectively, again conforming with chemical expectations. In 21 out of 32 cases, the EOS assignation can be considered as unquestionable (R = 100%). The worst case is given by the low-spin $Fe(CN)_6^{3-}$ complex, still with a pretty high R value of 85%. Let us analyze in more detail the eff-AO analysis for this species and the EOS assignation process. In Table 2, we collect the occupation number and types of all eff-AOs for both the alpha and beta parts. All six CN^- ligands are

DOI: 10.1021/ct501088v
J. Chem. Theory Comput. 2015, 11, 1501–1508

Table 1. *R* (%) Index Values for a Set of 32 Octahedral Complexes[a]

metal/ligands	Cl^- (HS)	H_2O (HS)	H_2O (LS)	CN^- (LS)	CO (LS)
V^{II}	100	100		99	100
Mn^{II}	100	100	100	97	100
Mn^{III}	87	100	100	95	93
Fe^{II}	100	100	100	99	97
Fe^{III}	100	100	100	85	91
Ni^{II}	100		100	98	100
Zn^{II}	100		100	99	100

[a]HS and LS stand for high-spin and low-spin, respectively. Roman superindices indicate the formal oxidation state of the TM atom.

Table 2. Full eff-AO Analysis for the $Fe(CN)_6^{3-}$ Complex[a]

eff-AO type	λ^α	eff-AO type	λ^α	eff-AO type	λ^β	eff-AO type	λ^β
Fe		C		Fe		C	
1s	1.000	1s	0.996	1s	1.000	1s	0.996
2s	1.000	2s	**0.694**	2s	1.000	2s	0.708
2p	1.000	2p	*0.235*	2p	1.000	2p	*0.246*
2p	1.000	2p	*0.232*	2p	1.000	2p	*0.239*
2p	1.000	2p	*0.153*	2p	1.000	2p	*0.153*
3s	0.991		*0.014*	3s	0.990		*0.015*
3p	0.983		*0.013*	3p	0.982		
3p	0.983			3p	0.982		
3p	0.982			3p	0.982		
3d	0.876	N		3d	0.827	N	
3d	0.848	1s	1.000	3d	0.827	1s	1.000
3d	0.848	2s	0.997	3d	***0.305***	2s	0.997
3d	***0.344***	2p	0.728	3d	*0.263*	2p	0.729
3d	*0.314*	2p	0.703	3d	*0.099*	2p	0.702
4s	*0.103*	2p	0.701	4s	*0.049*	2p	**0.665**
	0.050		*0.020*		*0.048*		*0.021*
	0.050				*0.048*		
	0.049				*0.032*		

[a]The frontier eff-AOs for each spin case are marked in bold (last occupied) and bold italic (first unoccupied). Unoccupied eff-AOs are marked in italic.

symmetry equivalent; hence, the type and occupation number of the eff-AOs are given for one representative C and N atom. The orbital type is determined by inspection of the eff-AOs obtained for each atom.

The EOS for this system are obtained as follows. There are 54 alpha electrons that need to be distributed among the set of alpha eff-AOs. After sorting the alpha eff-AOs by decreasing occupation number, 12 alpha electrons are assigned to the Fe atom, 5 to each of the six N atoms (30), and 2 to each of the C atoms (12). The last occupied overall alpha eff-AO belongs to either one of the six C atoms, with $\lambda^\alpha_{LO} = 0.694$. The first unoccupied alpha eff-AO is a d-type orbital of the Fe atom, with $\lambda^\alpha_{FU} = 0.344$. The corresponding value of the R_α index is 85%. For the beta part, there are 53 electrons. An analogous procedure assigns 11 electrons to the Fe atom, 5 to each of the six N atoms (30), and 2 to each of the six C atoms (12). The last occupied overall beta eff-AOs belong now to a N atom, with $\lambda^\beta_{LO} = 0.665$, whereas the first unoccupied is again a d-type orbital on the Fe atom with $\lambda^\beta_{FU} = 0.305$. The R_β (%) index amounts to 86%, so the overall *R* value for the EOS analysis is 85%. Finally, considering only the occupied eff-AOs, the electron configuration of the central Fe atom is $[Ar]3d^5 4s^0$, which corresponds to a (low-spin) Fe^{III} oxidation state for the Fe atom, as expected. For the N and C atoms, the effective electronic configurations are $1s^2 2s^2 2p^6$ and $1s^2 2s^2 2p^0$, respectively, which correspond to formal $N^{(3-)}$ and $C^{(2+)}$, and an overall $CN^{(-)}$.

As mentioned above, the eff-AO analysis relies on a definition of atom in the molecule. In order to check how dependent are the EOS on the particular atom in molecule definition, we have performed a systematic analysis for the 10 octahedral iron complexes of Table 1 using different atomic definitions, namely, Hilbert-space Mulliken's[8,12,29] and Löwdin's (see the Appendix), Bader's QTAIM,[13,22,30] and several fuzzy atom schemes such as Hirshfeld,[31] Hirshfeld-Iterative,[32] and the simplest Becke atoms.[33] The results are gathered in Tables S1−S10 of the Supporting Information. The EOS obtained are independent of the particular atomic definition in all cases but for $FeCN_6^{-3}$ using Becke atoms, where the alpha population of a d-type orbital of Fe atom competes with that of the 2p-type hybrid on all N atoms. As a result, the *R* index for a Fe^{III} oxidation state is slightly below 50% for the alpha part. On the other hand, the *R* values do differ significantly from one atom in molecule definition to another. Best performing approaches (in terms of higher *R* (%) values) are QTAIM, TFVC, and Hirshfeld-Iterative. It is worth remarking that for the simplest Becke atoms the relative size of each pair of bonded atoms is given by a fixed set of atomic radii. As the same atoms are treated on equal footing in different chemical environments, the partial ionic character of the bonds is not well captured by the Becke approach.[15] This problem is solved in the TFVC approach (and in QTAIM) as the relative atomic size is established by the position of the extrema of the density (usually a minimum) between the two atoms. A similar argument can be put forward for the classical Hirshfeld approach; the iterative version gives the necessary flexibility to describe the larger partial ionic character of the atoms. Mulliken-type results are comparable to Hirshfeld, but they are not recommended for EOS assignation, as the occupation numbers of the spin-resolved eff-AOs are not strictly restricted to the [0, 1] range. Moreover, it is well know that Mulliken-type approaches suffer from basis set dependencies. For this analysis, we have used a medium-sized basis set (6-31G*) with marked atomic character. Experience indicates that, contrary to the 3D-space approaches, the Mulliken-type results cannot be extrapolated to a larger basis such as the cc-pVTZ one. A much better alternative would be the Löwdin-type approach, which is expected to temper the basis set effects and where the occupation numbers do conform to the [0, 1] range. We can conclude that for EOS analysis atomic definitions that better take into account bond polarization are the most appropriate ones. Because of its simplicity, we recommend the use of the TFVC scheme.

On the other hand, the hierarchical fragment approach is illustrated by a number of isolated hexacoordinated [Fe(Pytacn)] complexes that are involved in C−H catalytic hydroxylation cycles, where the presence of Fe^V species has been postulated.[34] The tetradentate ligand Pytacn stands for 1-(2-pyridylmethyl)-4,7-dimethyl-1,4,7-triazacyclononane. The remaining two coordination positions are occupied by oxygen-containing ligands such as aquo, hydroxo, or oxo, formally considered as $H_2O^{(0)}$, $OH^{(1-)}$, and $O^{(2-)}$ species. The structures of the five [Fe(Pytacn)] active species are depicted in Figure S1 of the Supporting Information. All structures were fully optimized at the UB3LYP/SDD+6-311G(d,p) level of theory.[35]

DOI: 10.1021/ct501088v
J. Chem. Theory Comput. 2015, 11, 1501−1508

The complexes studied and the results of the EOS analysis are listed in Tables 3 and 4.

Table 3. Partial Charge (q) and Spin Populations (ρ_s) Using TFVC on the Fe Atoms for the [Fe(Pytacn)] Complexes

complex	q	q ideal	ρ_s	ρ_s ideal
$[Fe(Pytacn)(H_2O)_2]^{2+}$	1.28	+2	*a*	*a*
$[Fe(Pytacn)(H_2O)(OH)]^{1+}$	1.24	+2	*a*	*a*
$[Fe(Pytacn)(OH)_2]^{1+}$	1.68	+3	4.10	5
$[Fe(Pytacn)(OH)_2]^{2+}$	1.51	+4	1.88	2
$[Fe(Pytacn)O(H_2O)]^{2+}$	1.45	+4	1.30	2
$[Fe(Pytacn)O(OH)]^{1+}$	1.52	+4	3.14	4
$[Fe(Pytacn)O(OH)]^{2+}$	1.50	+5	2.10	3

[a]Spin-restricted calculation.

Table 4. Lowest Occupied and Highest Unoccupied Populations and R (%) Index for a Number of [Fe(Pytacn)] Complexes

oxidation states	$\lambda^{\alpha}_{LO}/\lambda^{\alpha}_{HU}$	$\lambda^{\beta}_{LO}/\lambda^{\beta}_{HU}$	R (%)
Fe^{II} bis aquo	0.80/0.15		100
Fe^{II} aquo, hydroxo	0.81/0.16		100
Fe^{III} bis hydroxo	0.86/0.12	0.78/0.24	100
Fe^{IV} bis hydroxo	0.59/0.44	0.71/0.33	65
Fe^{IV} oxo, aquo	0.67/0.37	0.53/0.38	65
Fe^{IV} oxo, hydroxo	0.56/0.52	0.61/0.32	54
Fe^{V} oxo, hydroxo	0.55/0.50	0.46/0.46	50

Neither the charges (q) nor the spin densities (ρ_s) on the Fe atom can be safely used to the recognize the OS of the metal. The small differences in the partial charge of the Fe atom among all species are particularly noticeable. Whereas formally the Fe atom is found in oxidation states from (II) to (V), the partial charges obtained are in the narrow range of +1.24 to +1.68. Moreover, the partial charge for the formally Fe(III) species $[Fe(Pytacn)(OH)_2]^{1+}$ is even larger (+1.68) than any of those found for the formally Fe(IV) and Fe(V) species. Conversely, the EOS analysis using the hierarchical fragment approach yields in all cases the chemically expected OS for the central Fe atom, as well as for the individual ligands, i.e., $Pytacn^{(0)}$, $aquo^{(0)}$, $hydroxo^{(1-)}$, and $oxo^{(2-)}$, independent of the spin state and even for the spin-restricted calculations.

The R values decrease as the OS of the metal increases, indicating that the formal picture of the high-valent species is farther from the actual electron distribution than for the low-valent ones. This is actually expected because the "charges" associated with the OS are only ideal, and the higher the oxidation state the more the actual atomic populations deviate from the formal ones.

It is worth analyzing in deeper detail the high-valent high-spin $[Fe(Pytacn)O(OH)]^{2+}$ species. The EOS analysis yields a high-valent Fe^{V} species, but the R indices for the alpha (R_α = 55%) and beta (R_β = 50%) contributions are rather low, indicating a significant Fe(IV)−oxyl character. This is given by the beta electron distribution, as the pseudodegenerate frontier eff-AOs with λ^{β} = 0.46 belong to the valence shell of the oxo group and a d-type hybrid on the Fe atom. Nevertheless, we find it remarkable that the EOS analysis still recognizes the high-valent high-spin d^3 iron species with strong Fe^{V} character, taking into account the values of the charge and spin densities of the metal atom and ligands obtained at this level of theory.

Indeed, in the ideal high-spin $Fe^{V}{=}O^{(2-)}$ picture (see Figure 1), the spin density on the Fe atom should be close to 3 and

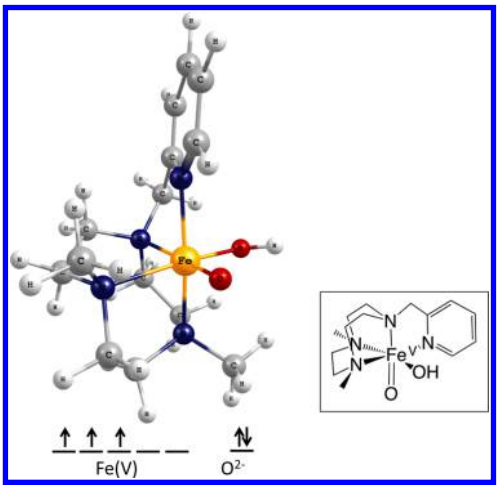

Figure 1. Ideal atomic orbital occupations for a high-spin $Fe^{V}{=}O^{(2-)}$ electron distribution.

that of the oxo moiety close to zero, as anticipated for a closed-shell oxo species. For this complex and at this level of theory, the spin density on the Fe atom amounts to only 2.10, whereas a significant value of 0.85 is found on the oxo moiety. Thus, the assignation of oxidation states based on the analysis of the spin density would probably point toward an iron(IV)-oxyl picture for this system. The advantage of the EOS analysis introduced here is that the atomic/fragment populations and spin densities are essentially analyzed in terms of individual effective orbital contributions. To illustrate this point, in Table 5, we gather the

Table 5. d-Type eff-AO Occupations of the Fe Atom in the $[Fe(Pytacn)O(OH)]^{2+}$ Species[a]

	σ			λ^{σ}	
α	**0.934**	**0.932**	**0.930**	0.495	0.451
β	0.163	0.393	0.462	0.322	0.349
$\alpha - \beta$	0.771	0.539	0.468	0.173	0.102

[a]Occupied eff-AOs are in boldface type.

occupations of the five d-type eff-AOs obtained for the central Fe atom. The alpha and beta eff-AOs have been matched by visual inspection. The EOS analysis indicated that only the first three alpha d-type eff-AOs are considered occupied.

The difference in the occupation numbers between these alpha and beta eff-AOs amounts to 2.05, very close to the overall spin density on the Fe atom (the numbers slightly differ because we consider only a subset of eff-AOs and also the occupation numbers are *net* populations). Thus, on average, there are two more alpha electrons on the Fe atom, but it can be readily seen that most of this spin population originates from the different alpha and beta occupation of *three* d-type eff-AOs, thus conforming with the ideal chemical picture of Figure 1.

Transition state structures are arguably the most challenging systems, as the conventional rules for formal electron counting are rather ambiguous. We further illustrate the new approach with the TS structure depicted in Figure 2. It corresponds to the H-abstraction step of the catalytic hydroxylation of cyclohexane with the [Fe(Pytacn)] complex, described at the UB3LYP/SDD+6-311G(d,p) level of theory. As described in

DOI: 10.1021/ct501088v
J. Chem. Theory Comput. 2015, 11, 1501−1508

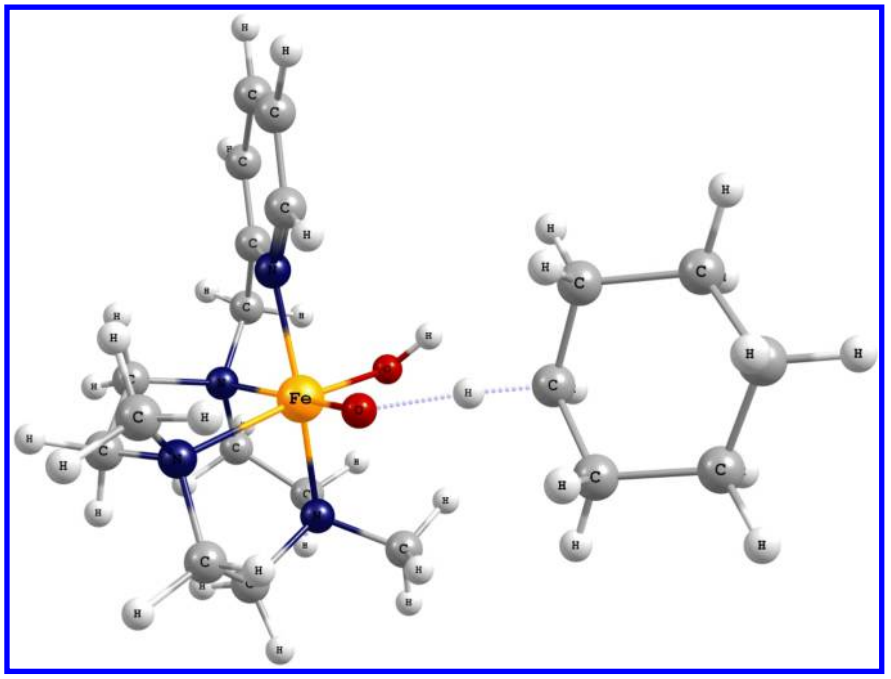

Figure 2. Transition state for the H-abstraction step of the catalytic hydroxylation of cyclohexane with [Fe(Pytacn)] catalyst (global charge +2, $\langle \hat{S}^2 \rangle$ = 3.80).

detail by Prat et al.,[35] in this step, a cyclohexane molecule interacts with the oxo group of the high-valent active species $[Fe^{V}(Pytacn)O(OH)]^{2+}$ (last structure in Table 4), and a H is transferred to the catalyst. In the gas phase, upon the formation of the OH bond, the reaction proceeds directly toward the formation of cyclohexanol and the $[Fe^{III}(Pytacn)(OH)]^{2+}$ species.

For the EOS analysis of the TS structure, different fragment definitions can be used. The H moeity is not yet fully transferred to the oxo group, so besides Fe and Pytacn, one can consider either two OH ligands and a cyclohexyl moiety (option A) or a cyclohexane fragment and the catalyst formally in the [Fe(Pytacn)O(OH)] form (option B). Furthermore, one could also consider the latter as cyclohexyl and an independent H center, thus defining six fragments. The results of the EOS analysis for the three alternatives are gathered in Table 6. The

Table 6. EOS and R_σ Values for Different Fragment Definitions for the TS Structure of Figure 2

fragments A	EOS	fragments B	EOS	fragments C	EOS
Fe	+4	Fe	+4	Fe	+4
Pytacn	0	Pytacn	0	Pytacn	0
OH	−1	OH	−1	OH	−1
O	−1	OH	−1	O	−2
C_6H_{12}	0	C_6H_{11}	0	C_6H_{11}	0
				H	+1
R_α = 71%, R_β = 59%		R_α = 62%, R_β = 75%		R_α = 62%, R_β = 61%	

fragment analysis clearly identifies in both cases the Ptacyn and one hydroxyl group as spectator ligands. Moreover, a Fe(IV) species, that lies between the oxidation states of reactants and products, is also obtained in all cases, as could be foreseen. In fact, one could also consider merely two fragments, namely, the Fe and the remaining centers. The EOS analysis again yields the metal with a formal oxidation state of +4.

The differences between fragment definitions lie in the EOS of the fragments/atoms directly involved in the bond breaking/formation, which gives different pictures of the reactive process, as illustrated in Figure 3. The R values (and even both R_α and

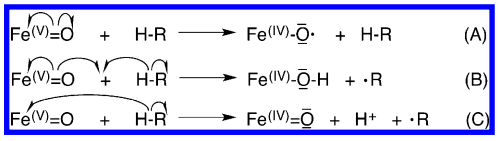

Figure 3. Arrow-pushing diagrams leading to bond patterns and EOS for options A, B, and C (see text).

R_β in borderline situations) can help to pick one or another fragmentation pattern, but one should typically expect rather low R values for these ambiguous cases. Clearly, other analysis tools more focused on chemical bonding like bond order analysis are better designed to decide whether a bond should be considered broken or not. Once this has been established, the EOS method provides the most appropriate formal picture derived from the actual electronic distribution, which has a special chemical significance in the case of transition metals.

For this example, when the H is still considered part of a cyclohexane fragment (option A), the EOS analysis points to a Fe(IV)−oxyl picture, which is also partially present in the reactant species discussed above. The EOS analysis describes the iron-oxo moiety activation with the oxyl formation, which is clearly associated with the observed iron−oxo bond elongation (1.706 Å vs 1.628 Å in the TS structure and the $[Fe^{V}(Pytacn)$-$O(OH)]^{2+}$ reactant, respectively). The R_β value is however the lowest one. For the fragment definition C, the analysis points toward the presence of an oxo species and an independent proton transferring from a neutral cyclohexyl moiety. The corresponding unusual arrow-pushing picture in Figure 3C indicates that, formally, iron would gather an e− from the H−C bond. However, both R_α and R_β values for option C are small, likely ruling out the presence of a formal oxo group in the TS

DOI: 10.1021/ct501088v
J. Chem. Theory Comput. 2015, 11, 1501−1508

structure. On the other hand, option B yields the larger values for the *R* indices. Accordingly, the TS structure is probably best characterized by the picture shown in Figure 3B, where the proton has already been transferred to the oxo group, forming a hydroxyl, and again a neutral-radical cyclohexyl.

Finally, it is worth stressing that the EOS analysis can be equally applied formally to any chemical species. In order to search for the limit of applicability of the present approach, we have computed the EOS for a set of organic and inorganic molecules. The results are collected in Table S11 of the Supporting Information. All species have been fully optimized at the B3LYP/cc-pVTZ level of theory. The eff-AOs have been obtained at the same level of theory using the TFVC atomic definition.

For the first set of compounds, the *R* values are very high. In all oxygen-containing species, we obtain formal $O^{(2-)}$ for the oxygen atom. In the set of second- and third-row hydrides, the OS of the hydrogen atom may be either (1+) or (1−), depending on the nature (and electronegativity) of the heteroatom. The *R* values are again very high except for H_2S (R = 55%), were the S atom is in fact predicted to be formally closer to $S^{(2+)}$. The H−S bonds are highly apolar; therefore, the formal view of separated charges is quite far from the actual electronic structure of the species. In fact, for such a small system already the simplest population analysis determines the outcome of the EOS calculation. We have found that partial charges on S are predicted either positive (QTAIM, TFVC, Löwdin) or negative (Hirshfeld, Hirshfeld-Iterative, Becke, Mulliken), and for partial charges below +0.10, the formal oxidation state predicted for S is (2−).

As could be anticipated, the worst scenario for the method are species exhibiting highly apolar bonds such as C−H and C−C ones. The *R* values for the set of hydrocarbons are around 50% (and even below) basically because the population of the 1s-type eff-AO on H atoms is comparable to that of the carbon's valence hybrids. There is no clear-cut distinction between proton and hydride assignation. These compounds and very apolar ones indicate the limit of applicability of the method. Nevertheless, for hydrocarbons and such highly apolar compounds, the formal OS are doubtful and have probably little relevance in most chemical applications. Of course, the hierarchical approach discussed above can still be invoked. For instance, methyl groups or $(CH)_n$ moieties in general may be chosen if necessary as fragments, so that the apolar C−H bonds are not formally broken in the EOS analysis.

7. CONCLUSIONS

In summary, we have introduced a simple and general method to compute oxidation states from electronic structure calculations. The analysis produces atom/fragment electronic configurations and a global index (*R*) that quantifies how close the overall OS assignation is to the actual electronic structure of the molecule. The method can be applied in equal footing for any system, level of theory, and even in the absence of atom-centered basis sets. A hierarchical scheme in which the system is first partitioned into fragments appears more appropriate for practical applications of complex systems. In general, low *R* values are expected for challenging cases such as transition state structures or highly apolar systems. For the former, when different fragment definitions may be applied, the *R* values, combined with other bond analysis tools, can still be used to determine the most suitable fragmentation pattern in order to extract a formal picture from the actual electronic distribution.

APPENDIX

A.1. Effective Atomic Orbitals for Löwdin Population Analysis

In the framework of Hilbert-space analysis, the effective atomic orbitals (hybrids)[8] for a given center or fragment *A* can be obtained by diagonalization of the $\mathbf{P}^A\mathbf{S}^A$ matrix,[36] where $\mathbf{P}^A$ and $\mathbf{S}^A$ are the $m_A \times m_A$ intra-atomic blocks of AO matrices **P** and **S**. In the Löwdin orthogonalized basis, the elements of the **P** matrix are expressed as

$$P^L_{\mu\nu} = [\mathbf{S}^{1/2}\mathbf{P}\mathbf{S}^{1/2}]_{\mu\nu} \tag{7}$$

Since the Löwdin basis is orthogonal, the eff-AOs associated with a given center *A* are simply obtained by solving the $m_A \times m_A$ eigenvalue equation

$$\mathbf{P}^{L,A}\mathbf{c}_i^{L,A} = \lambda_i^{L,A}\mathbf{c}_i^{L,A} \tag{8}$$

where $\mathbf{P}^{L,A}$ refers again to the intra-atomic block of the **P** matrix in the Löwdin basis.

One obtains up to m_A eigenvalues $\lambda_i^{L,A}$, where the non-zero ones correspond to the occupation numbers of the eff-AOs. Since there is no "net" population in the Löwdin basis, the occupation numbers of the eff-AOs of a given atom add up to its Löwdin population, similarly to real-space analysis with disjoint atomic domains (e.g., QTAIM). Moreover, it can be seen that, unlike the Mulliken-type approach, the occupation numbers of the spin-resolved eff-AOs are in the range $0 \le \lambda_i^{L,A} \le 1$. Unfortunately, the eff-AOs of a given atom are no longer expressed in terms of the original AOs centered on it but formally expanded over the whole AO basis set.

Finally, it is worth recalling that conventional Löwdin analysis is not rotationally invariant, unless the AO basis uses pure spherical harmonics or the AOs of each center are orthogonalized before the transformation.[37,38]

ASSOCIATED CONTENT

Supporting Information

Influence of the atomic definitions upon the EOS analysis (Tables S1−S10), EOS analysis for a set of organic and inorganic compounds (Table S11), and geometries of all [Fe(Pytacn)] species. This material is available free of charge via the Internet at http://pubs.acs.org.

AUTHOR INFORMATION

Corresponding Author

*Phone: +34 972 418358. Fax: +34 972 418357. E-mail: pedro.salvador@udg.edu.

Funding

Financial help from projects CTQ2011-23441/BQU, UNGI08-4E-003, and SGR528 is acknowledged. E.R-C. acknowledges support from Grant No. AP2008-01231 and from CIG No. PCI09-GA-2011-294240. V.P. acknowledges support from Grant No. BES-2012-052801 and from CTQ2011-23156/BQU.

Notes

The authors declare no competing financial interest.

ACKNOWLEDGMENTS

We are grateful to Dr. E. Matito and Dr. J. M. Luis for stimulating discussions. We would like to thank the University of Guanajuato for Computational resources via the CONACYT-UGTO National Laboratory (Grant 123732).

DOI: 10.1021/ct501088v
J. Chem. Theory Comput. 2015, 11, 1501−1508

REFERENCES

(1) Jansen, M.; Wedig, U. *Angew. Chem., Int. Ed. Engl.* **2008**, *47*, 10026−10029.
(2) Aullón, G.; Alvarez, S. *Theor. Chem. Acc.* **2009**, *123*, 67−73.
(3) Thom, A. J. W.; Sundstrom, E. J.; Head-Gordon, M. *Phys. Chem. Chem. Phys.* **2009**, *11*, 11297−11304.
(4) Brown, I. D. *The Chemical Bond in Inorganic Chemistry: The Bond Valence Model*; Oxford Univ. Press: Oxford, U.K., 2002.
(5) Sit, P. H.-L.; Car, R.; Cohen, M. H.; Selloni, A. *Inorg. Chem.* **2011**, *50*, 10259−10267.
(6) Knizia, G. *J. Chem. Theory Comput.* **2013**, *9*, 4834−4843.
(7) Sit, P. H.-L.; Zipoli, F.; Chen, J.; Car, R.; Cohen, M. H.; Selloni, A. *Chem.—Eur. J.* **2011**, *17*, 12136−12143.
(8) McWeeny, R. *Rev. Mod. Phys.* **1960**, *32*, 335−369.
(9) Foster, J. P.; Weinhold, F. *J. Am. Chem. Soc.* **1980**, *102*, 7211−7218.
(10) Carpenter, J. E.; Weinhold, F. *J. Mol. Struct.: THEOCHEM* **1988**, *169*, 41−62.
(11) Reed, A. E.; Weinstock, R. B.; Weinhold, F. *J. Chem. Phys.* **1985**, *83*, 735−746.
(12) Mayer, I. *Chem. Phys. Lett.* **1995**, *242*, 499−506.
(13) Mayer, I. *Can. J. Chem.* **1996**, *74*, 939−942.
(14) Cioslowski, J.; Liashenko, A. *J. Chem. Phys.* **1998**, *108*, 4405−4412.
(15) Mayer, I.; Salvador, P. *J. Chem. Phys.* **2009**, *130*, 234106.
(16) Lu, W.; Wang, C.; Schmidt, M.; Bytautas, L.; Ho, K.; Ruedenberg, K. *J. Chem. Phys.* **2004**, *120*, 2629−2637.
(17) Laikov, D. N. *Int. J. Quantum Chem.* **2011**, *111*, 2851−2867.
(18) West, A. C.; Schmidt, M. W.; Gordon, M. S.; Ruedenberg, K. *J. Chem. Phys.* **2013**, *139*, 234107.
(19) Janowski, T. *J. Chem. Theory Comput.* **2014**, *10*, 3085−3091.
(20) Qian, X.; Li, J.; Qi, L.; Wang, C.-Z.; Chan, T.-L.; Yao, Y.-X.; Ho, K.-M.; Yip, S. *Phys. Rev. B* **2008**, *78*, 245112.
(21) Mayer, I.; Bakó, I.; Stirling, A. *J. Phys. Chem. A* **2011**, *115*, 12733−12737.
(22) Ramos-Cordoba, E.; Salvador, P.; Mayer, I. *J. Chem. Phys.* **2013**, *138*, 214107−214107−9.
(23) Ponec, R.; Ramos-Cordoba, E.; Salvador, P. *J. Phys. Chem. A* **2013**, *117*, 1975−1982.
(24) Alvarez, S.; Hoffmann, R.; Mealli, C. *Chem.—Eur. J.* **2009**, *15*, 8358−8373.
(25) Conejeros, S.; Moreira, I. d. P. R.; Alemany, P.; Canadell, E. *Inorg. Chem.* **2014**, *53*, 12402−12406.
(26) Frisch, M. J.; Trucks, G. W.; Schlegel, H. B.; Scuseria, G. E.; Robb, M. A.; Cheeseman, J. R.; Montgomery, J. A.; Vreven, T.; Kudin, K. N.; Burant, J. C.; Millam, J. M.; Iyengar, S. S.; Tomasi, J.; Barone, V.; Mennucci, B.; Cossi, M.; Scalmani, G.; Rega, N.; Petersson, G. A.; Nakatsuji, H.; Hada, M.; Ehara, M.; Toyota, K.; Fukuda, R.; Hasegawa, J.; Ishida, M.; Nakajima, T.; Honda, Y.; Kitao, O.; Nakai, H.; Klene, M.; Li, X.; Knox, J. E.; Hratchian, H. P.; Cross, J. B.; Bakken, V.; Adamo, C.; Jaramillo, J.; Gomperts, R.; Stratmann, R. E.; Yazyev, O.; Austin, A. J.; Cammi, R.; Pomelli, C.; Ochterski, J. W.; Ayala, P. Y.; Morokuma, K.; Voth, G. A.; Salvador, P.; Dannenberg, J. J.; Zakrzewski, V. G.; Dapprich, S.; Daniels, A. D.; Strain, M. C.; Farkas, O.; Malick, D. K.; Rabuck, A. D.; Raghavachari, K.; Foresman, J. B.; Ortiz, J. V.; Cui, Q.; Baboul, A. G.; Clifford, S.; Cioslowski, J.; Stefanov, B. B.; Liu, G.; Liashenko, A.; Piskorz, P.; Komaromi, I.; Martin, R. L.; Fox, D. J.; Keith, T.; Al-Laham, M. A.; Peng, C. Y.; Nanayakkara, A.; Challacombe, M.; Gill, P. M. W.; Johnson, B.; Chen, W.; Wong, M. W.; Gonzalez, C.; Pople, J. A. *Gaussian 03*, revision C.02; Gaussian, Inc.: Pittsburgh, PA, 2003.
(27) Salvador, P., Ramos-Cordoba, E. *APOST-3D program* (available upon request to authors); Universitat de Girona: Girona, Spain, 2012.
(28) Salvador, P.; Ramos-Cordoba, E. *J. Chem. Phys.* **2013**, *139*, 071103.
(29) Mulliken, R. S. *J. Chem. Phys.* **1955**, *23*, 1833−1840.
(30) Bader, R. F. W. *Atoms in Molecules: A Quantum Theory*; Oxford Univ. Press: Oxford, U.K., 1990.
(31) Hirshfeld, F. *Theor. Chim. Acta* **1977**, *44*, 129−138.
(32) Bultinck, P.; van Alsenoy, C.; Ayers, P.; Carbó-Dorca, R. *J. Chem. Phys.* **2007**, *126*, 144111.
(33) Becke, A. *J. Chem. Phys.* **1988**, *88*, 2547−2553.
(34) Fillol, J. L.; Codolà, Z.; Garcia-Bosch, I.; Gómez, L.; Pla, J. J.; Costas, M. *Nat. Chem.* **2011**, *3*, 807−813.
(35) Prat, I.; Company, A.; Postils, V.; Ribas, X.; Que, L.; Luis, J. M.; Costas, M. *Chem.—Eur. J.* **2013**, *19*, 6724−6738.
(36) Mayer, I. *J. Phys. Chem.* **1996**, *100*, 6249−6257.
(37) Mayer, I. *Chem. Phys. Lett.* **2004**, *393*, 209−212.
(38) Bruhn, G.; Davidson, E. R.; Mayer, I.; Clark, A. E. *Int. J. Quantum Chem.* **2006**, *106*, 2065−2072.

DOI: 10.1021/ct501088v
J. Chem. Theory Comput. 2015, 11, 1501−1508